Proceedings of the 17th World Congress
The International Federation of Automatic Control
Seoul, Korea, July 6-11, 2008

On the transfer properties of second-order sliding mode control systems

Igor Boiko * **Leonid Fridman** ** **Alessandro Pisano** *** **Elio Usai** ***

* *University of Calgary, Canada. e-mail: i.boiko@ieee.org.*
** *Dep.to de Control, Facultad de Ingeniería, National Autonomous University of Mexico, Mexico. e-mail: lfridman@servidor.unam.mx*
*** *Dept. of Electrical and Electronic Engineering, University of Cagliari, 09123 Cagliari, Italy. e-mail: {giob,amuntoni,pisano,eusai}@diee.unica.it).*

Abstract: A comprehensive approach to the input/output analysis of a class of second-order sliding mode control (2-SMC) systems is developed. Linear SISO plants with the "generalized suboptimal" 2-SMC algorithm are investigated. It is shown that in order to evaluate the properties of robustness against the presence of external perturbations the generalized suboptimal controller can be replaced by a proper constant gain, which is called "equivalent gain". The approximate DF method, and the theoretically exact LPRS method, are developed for computing the equivalent gain. It results from the presented analysis that the considered algorithm possesses an higher equivalent open-loop gain as compared to the standard relay. A thoroughly discussed worked example confirms the theoretical results and shows the feasibility of the presented procedures.

1. INTRODUCTION

Discontinuous control systems are the oldest, and one of the most widespread, type of nonlinear control systems, see Hawkins (1887). It was clearly recognized that discontinuous control systems provides several advantages over the linear ones principally due to: simplicity of design, cheaper components, and the ability to maintain satisfactory performance as the parameters of the system change, see Gelb et al. (1968).

The theory of discontinuous control is generally considered as a rather mature subject. However, many problems, especially related to periodic motion analysis, still remain open. One of them is the analysis of the *transfer properties* of the discontinuous control system, the knowledge of which is extremely important in the real applications, that is going to be introduced later on.

There is a fundamental distinction in that periodic motions can be autonomous (i.e., self sustained) or induced by external signals. The majority of the literature on discontinuous control systems studied autonomous periodic modes, whilst much less studies have been devoted to the periodic motions affected by exogenous signal. The exogenous signals may include measured or unmeasured disturbances as well as reference signals.

The servo aspect of discontinuous control is very important and seemed underestimated in the past literature. The knowledge of input-output properties is as important as the knowledge of the autonomous behaviour (self-excited oscillations) in discontinuous control systems. In fact, those two aspects complement each other. For example, in designing an on-off room temperature control system it is equally important to know what the frequency of the relay switching will be (autonomous behaviour) as well as how the average temperature would change under the effect of the changing outside temperature. The latter problem can be solved only if the transfer properties of the systems are considered.

Let us understand by the *transfer properties analysis* the problem of investigating the system response to an external signal, says f_0, which can represent a disturbance, which the system is supposed to reject, or a reference input, which the system is supposed to track. Clearly, this is an extension of the autonomous mode analysis, the latter being included as a special case corresponding to $f_0 = 0$.

The main contribution of this work is the full development of frequency-domain techniques of analysis of the input-output properties of a class of second-order sliding mode control (2-SMC) systems, see Emelyanov et al. (1993) and Levant (1993). The present treatment is developed by considering the "Generalized Sub-optimal" (G-SO) algorithm, a relay with modified switching function, see Bartolini et al. (1999) and Bartolini et al. (2003).

The essence of the presented input-output analysis is the replacement of the discontinuous 2-SMC element with a certain, properly computed, constant gain called "equivalent gain". This replacement makes it possible to evaluate the transfer properties of the system by using standard transfer function algebra and frequency-response analysis.

For linear plants with dynamic actuators and the G-SO algorithm in the closed loop, we present two distinct frequency-based approaches to compute the equivalent gain:

- An approximate method based on the Describing Function (DF) concept, see Gelb et al. (1968)
- An exact method based on the concept of the Locus of a Perturbed Relay System (LPRS), see Boiko (2005)

The paper is organized as follows. Section 2 recalls some useful related results and formulates the main problem under analysis. In Sections 3 and 4 the two distinct approaches to the input/output analysis (DF and LPRS based) are described. The conclusive Section 5 demonstrates the proposed methods by means of worked simulation examples.

2. FREQUENCY-DOMAIN ANALYSIS OF 2-SMC SYSTEMS

Consider a linear asymptotically stable system controlled by the generalized sub-optimal algorithm to which an external *constant* input f_0 is applied as in Fig. 1.

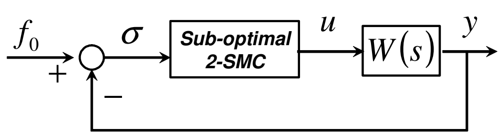

Fig. 1. 2-SMC system with an external input

The generalized sub-optimal algorithm takes the following form

$$u = -U\mathrm{sign}\left(\sigma - \beta\sigma_{Mi}\right) \tag{1}$$

where U and β are the constant controller parameters and σ_{Mi} is the latest "*singular point*" of σ, i.e., the value of σ at the most recent time instant t_{Mi} $(i = 1, 2, \ldots)$ such that $\dot{\sigma}(t_{Mi}) = 0$.

2.1 Review of autonomous properties analysis

The autonomous properties of the above system (i.e., the resulting behaviour with $f_0 = 0$) were investigated recently in Boiko et al. (2006) and Boiko et al. (2007). It was shown that if the transfer function $W(s)$ has input-output relative degree on three, or more, then the system may feature stable steady state periodic oscillations.

In Boiko et al. (2006) it was derived a simple DF-based graphical procedure for computing approximately the values of the frequency Ω_p and amplitude σ_M^p of the periodic motion that can occur in the above system when $f_0 = 0$. The frequency and amplitude of the periodic motion are estimated by solving the complex "harmonic balance" equation Atherton (1975)

$$W(j\Omega_p) = -\frac{1}{q(\sigma_M^p)} \tag{2}$$

with the DF negative reciprocal, which is a function of the unknown oscillation amplitude σ_M^p, taking the following form

$$-\frac{1}{q(\sigma_M^p)} = -\frac{\pi\sigma_M^p}{4U}\left(\sqrt{1-\beta^2} - j\beta\right) \tag{3}$$

From a graphical point of view, the harmonic balance equation entails finding the intersection point P of the two loci in the complex plane (see Figure 2). Therefore, a periodic motion may occur if at some frequency $\omega = \Omega_{DF}^p$ the phase characteristic of the transfer function $W(j\omega)$ (which may comprise the plant, actuator and sensor dynamics) is equal to $-180^0 - arcsin(\beta)$. If such a requirement is fulfilled, so that an intersection point P between the two loci occurs, then the frequency of the periodic solution is the "cross-over" frequency Ω_{DF}^p, while the oscillation amplitude is given by

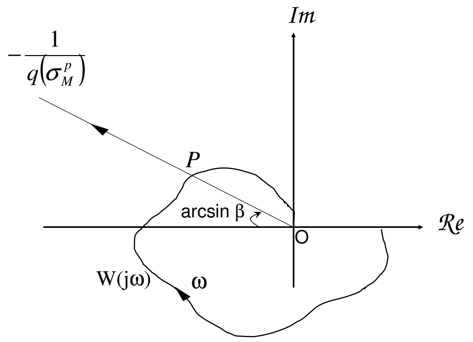

Fig. 2. DF analysis of self-excited oscillations

$$\sigma_{M,DF}^p = \frac{4U}{\pi}\|W(j\Omega_{DF}^p)\| \tag{4}$$

The subscript DF is added to stress that the present analysis involves the use of the describing function method. Clearly an intersection point out of the origin will exist if the overall relative degree of the combined actuator-plant-sensor relative degree is three or more.

The previous method gives only approximate values of the periodic solution parameters, and it is based on the filtering hypothesis. An exact method is suggested in Boiko et al. (2007). It is based on the following complex locus:

$$\Phi(\omega) = -\sqrt{[\sigma_M^p(\omega)]^2 - \sigma^2\left(\frac{\pi}{\omega},\omega\right)} + j\sigma\left(\frac{\pi}{\omega},\omega\right) \tag{5}$$

where

$$\sigma_M^p(\omega) = \max_{t\in[0,\frac{2\pi}{\omega}]}|\sigma(t,\omega)| \tag{6}$$

In order to implement the definition formula in practice the ω-periodic solution $\sigma(t,\omega)$ can be expressed by means of its Fourier series:

$$\sigma(t,\omega) = \frac{4U}{\pi}\sum_{k=1}^{\infty}\frac{1}{k}sin\left(\frac{1}{2}\pi k\right)sin[k\omega t + \arg W(jk\omega)]\|W(jk\omega)\| \tag{7}$$

It was shown in Boiko (2005) that function $\Phi(\omega)$ has the same imaginary part as the Tsypkin locus, see Tsypkin (1984). Having computed the function $\Phi(\omega)$, we can carry out the graphical analysis of possible periodic motions in the same way as it was done above via the DF technique, simply replacing the Nyquist plot of $W(j\omega)$ with that of the complex function $\Phi(\omega)$ given by (5), and computing the resulting point of intersection. The oscillation frequency Ω_{LPRS}^p is the crossover one, as in the DF-based procedure. The main difference is that in this case the amplitude of the oscillation coincides with the distance of the intersection point from the origin (no scaling like in (4) is necessary):

$$\sigma_{M,LPRS}^p = \|\Phi(\Omega_{LPRS}^p)\| \tag{8}$$

The more terms are included in computing the series (7), the more accurate is the result of the computation.

2.2 Transfer properties analysis

The statement of the problem of transfer properties analysis for the block scheme represented in the Figure 1 is the subject of the present subsection.

Let $f_0 \neq 0$ and assume that the output and error variables y and σ in the steady state are T-periodic, possibly asymmetric, signals. y and σ will be oscillating around f_0 and around the zero value, respectively. Denote as $a_p > f_0$ and $a_n < f_0$ the maximal and minimal amplitude of y.

The average value of σ is denoted as σ_0, and the maximal and minimal amplitude of σ are denoted as $\sigma_{max} > 0$ and $\sigma_{min} < 0$, respectively. Since $\sigma = f_0 - y$, it follows that

$$\sigma_{\min} = f_0 - a_p \tag{9}$$

$$\sigma_{\max} = f_0 - a_n \tag{10}$$

With such a periodic steady-state evolution of σ, we can replace the suboptimal algorithm by an asymmetric hysteretic relay (Fig. 3), with the following hysteresis values b_1 and b_2:

$$b_1 = -\beta\sigma_{min} \qquad b_2 = -\beta\sigma_{max} \tag{11}$$

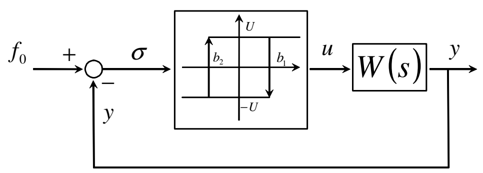

Fig. 3. The suboptimal algorithm as an asymmetric hysteretic relay.

In order to derive an equivalent representation having a *symmetric* hysteretic relay, a modified, shifted, error variable σ^* is considered, which is defined as follows

$$\sigma^*(t) = \sigma(t) - \Delta_\sigma \qquad \Delta_\sigma = \frac{b_2 + b_1}{2} \tag{12}$$

By considering σ^* as the input of the nonlinear element, the suboptimal algorithm can be actually replaced by a symmetric relay with the hysteresis value $b = \frac{b_1 - b_2}{2}$ and an additional input Δ_σ (Figure 4).

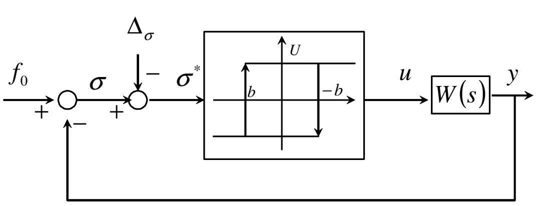

Fig. 4. The equivalent system with error augmentation (12)

In the steady state, the plant input $u(t)$ will be a T-periodic pulse-width modulated square wave signal with the positive and negative pulse duration θ_1 and θ_2 ($\theta_1 + \theta_2 = T$). The mean value u_0 of u is defined as follows:

$$u_0 = U\,\frac{\theta_1 - \theta_2}{\theta_1 + \theta_2} = \frac{2\theta_1 - T}{T}U \tag{13}$$

The average error σ_0 and the average control u_0 are both functions of the magnitude of the constant input f_0. Consider now the dependence of u_0 on σ_0, which will be referred to as the *bias function.* Simulations show that the bias function is close to linear in a wide range of f_0 variation. Then the following first-order Taylor approximation can be made

$$u_0 = k_n\sigma_0 \tag{14}$$

The gain k_n, the slope of the approximated bias function, is called equivalent gain for the average values, *equivalent gain* for brevity. The equivalent gain will be determined as the slope of the exact bias function $u_0 = u_0(\sigma_0)$ at the origin.

By approximating the bias function with a gain, we are able to analyze the propagation of the averaged system variables by standard linear analysis making reference to the scheme in Fig. 5. This result constitutes the core of the present method of analysis.

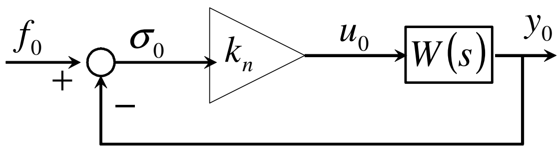

Fig. 5. The equivalent system for the averaged motion analysis

In the next sections two methods for computing the equivalent gain are suggested. The first method, the DF-based approach (Section 3), is based on the filtering hypothesis on $W(j\omega)$. The second method, the LPRS-based approach (Section 4) dispenses with the filtering hypothesis and gives a more accurate (theoretically exact) value of k_n.

3. DF BASED INPUT OUTPUT ANALYSIS

Let us compute the equivalent gain of the suboptimal algorithm by using the DF approach, i.e. considering only the fundamental harmonics of the periodic signals.

The following relationships occur between the hysteresis values b_1, b_2 in (11) and the amplitudes $\sigma_{\min}$, $\sigma_{\max}$, a_p, a_n of the signal oscillations:

$$b_1 = -\beta\sigma_{\min} = -\beta f_0 + \beta a_p \tag{15}$$

$$b_2 = -\beta\sigma_{\max} = -\beta f_0 + \beta a_n \tag{16}$$

By considering (15)-(16) into (12) it yields that Δ_σ is expressed as follows

$$\Delta_\sigma = -\frac{\beta}{2}\left(2f_0 - a_p - a_n\right) \tag{17}$$

The derivative $\frac{d\Delta_\sigma}{du_0}$ is therefore

$$\frac{d\Delta_\sigma}{du_0} = \frac{\beta}{2}\left(\frac{da_p}{du_0} + \frac{da_n}{du_0} - 2\frac{df_0}{du_0}\right) \tag{18}$$

The above derivative is to be evaluated at the point $u_0 = 0$. The derivative of u_0 with respect to θ_1, that will be used later on, can be computed easily from (13) and it is given by

$$\frac{du_0}{d\theta_1} = \frac{2U}{T} \quad \rightarrow \quad \frac{d\theta_1}{du_0} = \frac{T}{2U} \tag{19}$$

According to the filtering hypothesis, consider the first-order Fourier expansion of the asymmetric T-periodic control $u(t)$:

$$u(t) = u_0 + \frac{4U}{\pi}\sin(\pi\theta_1/(\theta_1+\theta_2)) \times \cos(\frac{2\pi}{T}(t-\theta_1/2)) \tag{20}$$

By propagating the input (20) through the plant transfer function one can express as follows the maximal and minimal values of y

$$a_p = u_0 W(j0) + \frac{4U}{\pi}\sin(\pi\theta_1/(\theta_1+\theta_2))\|W(j\Omega_p)\| \tag{21}$$
$$a_n = u_0 W(j0) - \frac{4U}{\pi}\sin(\pi\theta_1/(\theta_1+\theta_2))\|W(j\Omega_p)\| \tag{22}$$

where $\Omega_p = 2\pi/T$ is the frequency of the oscillation.

We can now compute the derivative terms in (18). Let us compute the derivative $\frac{da_p}{du_0}$ in the point $u_0 = 0$, i.e. letting $\theta_1 = \theta_2 = T/2$. After simple manipulations obtain

$$\frac{da_p}{du_0} = W(j0) + |W(j\Omega_p)|cos(\pi/2) = W(j0) \tag{23}$$

The same applies to the derivative of a_n, therefore we get

$$\left.\frac{da_p}{du_0}\right|_{u_0=0} = \left.\frac{da_n}{du_0}\right|_{u_0=0} = W(j0) \tag{24}$$

The remaining derivative term $\frac{df_0}{du_0}$ in (18) can be obtained from the balance equation of the average signal values in the considered system:

$$(f_0 - u_0 W(j0))k_{nDF} = u_0 \tag{25}$$

where k_{nDF} is the equivalent gain of the sub-optimal algorithm, **which we aim to find**. The subscript DF indicates that the present analysis involves the use of the describing function method.

Relationship (25) is rewritten as $f_0/u_0 = 1/k_{nDF} + W(j0)$, differentiating which one obtains

$$\frac{df_0}{du_0} = \frac{1}{k_{nDF}} + W(j0) \tag{26}$$

Considering (24) and (26) into (18) obtain the final form of $d\Delta_\sigma/du_0$:

$$\left.\frac{d\Delta_\sigma}{du_0}\right|_{u_0=0} = \beta W(j0) - \beta\left(\frac{1}{k_{nDF}} + W(j0)\right) = -\frac{\beta}{k_{nDF}} \tag{27}$$

Once the error augmentation term Δ_σ satisfy the formula (27), it makes sense to consider an approximate linear relationship between Δ_σ and u_0, obtaining the equivalent system representation as in Fig. 6, where the gain k^*_{nDF} is the equivalent gain of the symmetric hysteretic relay with the hysteresis value $b = \beta\sigma^p_{M,DF}$. k^*_{nDF} was derived in Boiko (2005) as:

$$k^*_{nDF} = \frac{2U}{\pi\sqrt{\left(\sigma^p_{M,DF}\right)^2 - b^2}} = \frac{2U}{\pi\sigma^p_{M,DF}\sqrt{1-\beta^2}} \tag{28}$$

It should be noted that the computation of the equivalent gain depends on $\sigma^p_{M,DF}$, then the amplitude of the self-sustained oscillations affect the transfer properties of the system. Thus the autonomous oscillations must be preliminarily studied using the methods previously described.

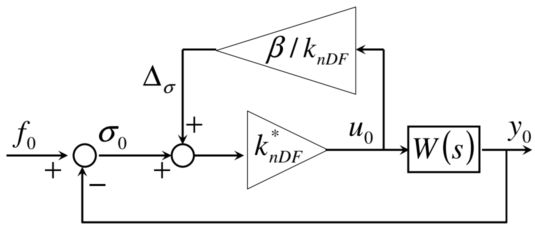

Fig. 6. The equivalent system for the averaged motion analysis

The equivalent gain k_{nDF} is by definition the ratio between u_0 and σ_0. It can be then obtained by referring to the scheme in Figure 6 and solving the inner feedback loop. It results the implicit relationship

$$k_{nDF} = \frac{u_0}{\sigma_0} = \frac{k^*_{nDF}}{1 - \beta k^*_{nDF}/k_{nDF}} \tag{29}$$

which yields to the following expression for the equivalent gain of the suboptimal algorithm:

$$k_{nDF} = k^*_{nDF}(1+\beta) = \frac{2U(1+\beta)}{\pi\sigma^p_{M,DF}\sqrt{1-\beta^2}} \tag{30}$$

The equivalent system of average values propagation can be depicted as in Fig. 7

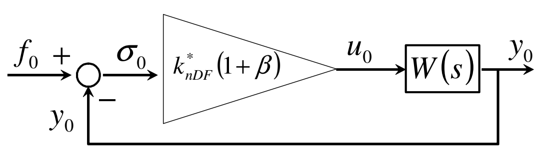

Fig. 7. Simplified equivalent system for averaged motion propagation analysys

Once the equivalent representation in Fig. 7 is achieved, the propagation of the input f_0 can be studied by classical linear frequency methods of analysis. The results will be reliable as long as the input signal f_0 will be characterized by frequency components well below the chattering frequency Ω_p.

Note that the application of the sub-optimal 2-SMC algorithm instead of the standard relay results in an increase of the equivalent gain. Such an increase is governed by the parameter β of the algorithm, the larger β the larger k_{nDF}.

4. LPRS BASED INPUT OUTPUT ANALYSIS

We now carry out the input-output analysis via the Locus of a Perturbed Relay System (LPRS) method, which takes into account the higher harmonics of the oscillation variables and is therefore theoretically exact without requiring any filtering assumption on the plant transfer function.

The following relationship holds by definition

$$\frac{d\sigma_0}{du_0} = \frac{1}{k_{nLPRS}} \tag{31}$$

with the subindex "LPRS" denoting the used approach. It follows from (12) that $\sigma_0 = \sigma_0^* + \Delta_\sigma$, differentiating which with respect to u_0 yields the following:

$$\frac{d\sigma_0}{du_0} = \frac{d\sigma_0^*}{du_0} + \frac{d\Delta_\sigma}{du_0} = \frac{1}{k^*_{nLPRS}} + \frac{d\Delta_\sigma}{du_0} \tag{32}$$

where k^*_{nLPRS} is the equivalent gain obtained via the LPRS for the equivalent system with symmetric relay having the hysteresis value $b = \beta\sigma^p_{M,LPRS}$.

The gain k^*_{nLPRS} was computed in Boiko (2005) as follows

$$k^*_{nLPRS} = \frac{1}{-2\,\mathtt{Re}\;[J(\Omega^p_{LPRS})]} \tag{33}$$

as a function of the LPRS $J(\omega)$ (see Boiko (2005)), which is defined by the following complex function

$$J(\omega) = \sum_{k=1}^{\infty}(-1)^{k+1}\mathtt{Re}W(k\omega) + j\sum_{k=1}^{\infty}\frac{\mathtt{Im}W((2k-1)\omega)}{2k-1} \tag{34}$$

Considering (31)-(33) it follows that the equivalent gain k_{nLPRS} that we are aimed to find will satisfy the following condition

$$\frac{1}{k_{nLPRS}} = -2\,\mathtt{Re}\;[J(\Omega^p_{LPRS})] + \frac{d\Delta_\sigma}{du_0} \tag{35}$$

The last term in eq. (35) was derived in the previous section and is reported again below

$$\frac{d\Delta_\sigma}{du_0} = -\frac{\beta}{2}\left(\frac{da_p}{du_0} + \frac{da_n}{du_0} - 2\frac{df_0}{du_0}\right) \tag{36}$$

Let us compute the terms $\frac{da_p}{du_0}$, $\frac{da_n}{du_0}$, $\frac{df_0}{du_0}$ appearing in (36).

a_p and $-a_n$ are the maximal and minimal values of the plant output y. In order to express $y(t)$ it must be considered the full Fourier expansion of the asymmetric periodic control $u(t)$ (in the previous section only the first harmonic term was considered), which must be propagated through the transfer function $W(j\omega)$. Skipping for brevity the series expression of $u(t)$, the output $y(t)$ turns out to be given as follows:

$$\begin{aligned} y(t) = y_0 + \frac{4U}{\pi}\sum_{k=l}^{\infty}\frac{1}{k}sin(\frac{k}{2}\Omega\theta_1)\times \\ \times\Big\{\cos(\frac{k}{2}\Omega\theta_1)\cos[k\Omega t + \arg W(jk\Omega)] + \\ + \sin(\frac{k}{2}\Omega\theta_1)\sin[k\Omega t + \arg W(jk\Omega)]\Big\}\,\|W(jk\omega)\| \end{aligned} \tag{37}$$

Now computing the derivative of $y(t)$ with respect to θ_1, evaluating it at $\theta_1{=}\pi/\Omega$, and making some manipulations, obtains

$$\begin{aligned} \frac{\partial y(t)}{\partial\theta_1} = \frac{\partial y_0}{\partial\theta_1} + \frac{2U}{\pi}\sum_{k=l}^{\infty}\Omega\,(-1)^k\,[\cos(k\Omega t)\cos\arg W(jk\Omega) \\ - \sin(k\Omega t)\sin\arg W(jk\Omega)]\|W(jk\Omega)\| \end{aligned} \tag{38}$$

Let $t = t_{max}$ be the time at which y reaches its maximum a_p. Then the minimum a_n will be reached at $t = t_{min} = t_{max} + \pi/\Omega$. By definition

$$\left.\frac{\partial y(t)}{\partial t}\right|_{t=t_{max}} = \left.\frac{\partial y(t)}{\partial t}\right|_{t=t_{min}} = 0 \tag{39}$$

The derivatives of a_p and a_n with respect to u_0 can be determined as follows by taking into account (19) and (39)

$$\frac{da_p}{du_0} = \frac{T}{2U}\left.\frac{\partial y(t)}{\partial\theta_1}\right|_{t=t_{max}} \tag{40}$$

$$\frac{da_n}{du_0} = \frac{T}{2U}\left.\frac{\partial y(t)}{\partial\theta_1}\right|_{t=\pi/\Omega+t_{max}} \tag{41}$$

The above derivative terms can be directly obtained from (38). After tedious but straightforward computations the following final expressions for $\frac{da_p}{du_0}$ and $\frac{da_n}{du_0}$ are derived:

$$\begin{aligned} \frac{da_p}{du_0} = \frac{dy_0}{du_0} + 2\sum_{k=l}^{\infty}(-1)^k\;[\cos(k\Omega t_{\max})\cos\arg W(jk\Omega) - \\ - \sin(k\Omega t_{\max})\sin\arg W(jk\Omega)]\cdot\|W(jk\Omega)\| \end{aligned} \tag{42}$$

$$\begin{aligned} \frac{da_n}{du_0} = \frac{dy_0}{du_0} + 2\sum_{k=l}^{\infty}[\cos(k\Omega t_{\max})\cos\arg W(jk\Omega) - \\ - \sin(k\Omega t_{\max})\sin\arg W(jk\Omega)]\cdot\|W(jk\Omega)\| \end{aligned} \tag{43}$$

Now, by considering (42) and (43), and taking into account that that $\frac{dy_0}{du_0} = W(j0)$, we can rewrite (36) in the final form as follows

$$\frac{\partial\Delta_\sigma}{\partial u_0} = -\beta\left\{-\frac{df_0}{du_0} + W(j0) + 2R(\Omega)\right\} \tag{44}$$

$$R(\Omega) = \sum_{k=l}^{\infty}[\cos(2k\Omega t_{\max} + \arg W(j2k\Omega))]\,\|W(j2k\Omega)\| \tag{45}$$

Function $R(\Omega)$ accounts for the unequal response of the negative and positive amplitudes to the change of u_0. It contains only even harmonics of the fundamental frequency component.

The derivative term df_0/du_0 in (44) can be written as follows by analogous steps as those made in the DF analysis:

$$\frac{df_0}{du_0} = \frac{1}{k_{nLPRS}} + W(j0) \tag{46}$$

Therefore we obtain that

$$\frac{\partial\Delta_\sigma}{\partial u_0} = \frac{\beta}{k_{nLPRS}} - 2\beta R(\Omega) \tag{47}$$

Now considering (47) into (35) and rearranging it yields the final formula for the equivalent gain using the LPRS method of analysis.

$$k_{nLPRS} = \frac{1+\beta}{-2\mathrm{Re}\,[J(\Omega^p_{LPRS})] + 2\beta R(\Omega^p_{LPRS})} \tag{48}$$

Like in the DF approach an increase of the equivalent gain value, in comparison with the relay control, arises due to the multiplier $(1+\beta)$.

5. SIMULATION EXAMPLES

Consider the simple system consisting of a spring-loaded cart moving on the inclined plane subject to viscous damping. The motion equations of the system are as follows

$$\begin{aligned} \dot{x}_1 &= x_2 \\ \dot{x}_2 &= -\frac{k}{M}x_1 - \frac{b}{M}x_2 + \frac{1}{M}u_a + gsin(\psi) \end{aligned} \tag{49}$$

with x_1 and x_2 being the trolley position and velocity variables, u_a the control force exerted on the cart, $M = 1kg$ the trolley mass, $k = 1Nm^{-1}$ the spring coefficient, $b = 1Nsm^{-1}$ the viscous friction coefficient, $\psi = 5deg$ the angle of inclination, and g the gravity term.

It is assumed that the control force u_a is generated through a dynamic actuator with the second order dynamics

$$T_a^2\ddot{u}_a + 2\xi T_a\dot{u}_a + u_a = u, \qquad T_a = 0.01s, \qquad \xi = 0.8 \tag{50}$$

The goal is to stabilize the cart in the point corresponding to zero displacement. To this end we can design the switching surface (line) $\sigma = x_1 + x_2 = 0$. Consider two different controllers, namely the simple relay

$$u = -4sign(\sigma) \tag{51}$$

and the generalized suboptimal controller with the same magnitude $U = 4$ and the anticipation factor $\beta = 0.3$:

$$u = -4\text{sign}\left(\sigma - 0.3\sigma_{Mi}\right) \tag{52}$$

Write an expression for the transfer function of the linear plant-actuator part of the control system

$$W_{u-\sigma}(s) = (s+1)W_a(s)W_p(s) \tag{53}$$

where $W_a(s)$ and $W(s)$ are the actuator and plant transfer functions, respectively

$$W_a(s) = \frac{1}{0.0001s^2 + 0.016s + 1}, \quad W_p(s) = \frac{1}{s^2+s+1} \tag{54}$$

The block scheme of the system under study, with the Suboptimal controller in the feedback loop, can be represented as in Fig. 8.

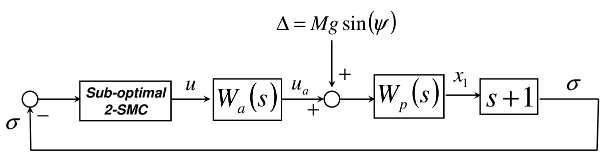

Fig. 8. Block scheme of the simulated system

The simultaneous presence of the actuator dynamics and of the constant disturbance $Mgsin(\psi)$ will cause a steady state motion of σ and x_1 characterized by a steady-steady constant error component plus a fast periodic oscillation. The tools developed in this paper allow a complete understanding and quantitative characterization of this phenomenon.

The first step of the analysis entails the study of the oscillations occurring in the autonomous (i.e., disturbance-free) closed loop system. The parameters of the autonomous oscillations of σ (obtained by means of the DF and LPRS methods according to the procedures described in Sect. 2) were computed for both the relay and suboptimal controller (see Fig. 9).

	Relay control		***Suboptimal Control***	
	Frequency [rad sec^{-1}]	Amplitude	Frequency [rad sec^{-1}]	Amplitude
DF	100	0.032	128	0.018
LPRS	98.8	0.033	126.4	0.019
Simulation	98.4	0.033	125.9	0.019

Fig. 9. Analysis of the autonomous periodic motion with relay and suboptimal control.

Let us study the propagation of the gravity disturbance. Figures 10 show the steady state behaviour of x_1 for both controllers. Denote as x_{10} the steady state average value of the signal.

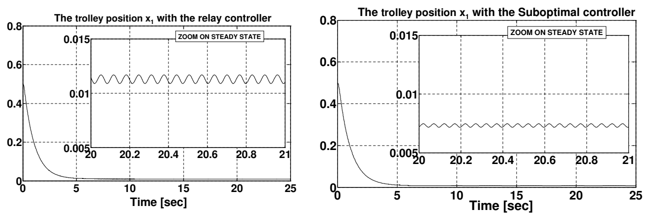

Fig. 10. Trolley position in the considered example. Left: relay control. Right: Suboptimal control

The expected value of x_{10} is obtained by linear system analysis after that the controller is replaced by its equivalent gain.

$$x_{10} = \frac{gsin(\psi)}{1+k_n} = \frac{0.85}{1+k_n} \tag{55}$$

Now let us compute the equivalent gains of the relay and suboptimal controllers. Notice that the analysis of the relay controller, firstly presented in Boiko (2005), is contained as a particular case ($\beta = 0$) of the general procedure presented in this work.

The equivalent gain formula derived using the DF approach was given in (30). For the relay, it must be set $\beta = 0$ and $\sigma^p_{M,DF} = 0.032$. It yields $k_{nDF} = 79.5$. For the suboptimal algorithm, the values $\beta = 0.3$ and $\sigma^p_{M,DF} = 0.018$ must be considered, which yield $k_{nDF} = 187.5$.

The equivalent gain formula using the LPRS approach was given in (48). For the relay, it must be set $\beta = 0$ and we have that $\Omega^p_{LPRS} = 98.8$ and $ReJ(98.8) = -0.0057$, which implies that $k_{nLPRS} = 76.9$. For the suboptimal algorithm, the value $\beta = 0.3$ must be considered. We have that $\Omega^p_{LPRS} = 126.4$. Since $ReJ(126.4) = -0.0033$ that $R(126.4) = 4.78e-4$, it yields $k_{nLPRS} = 188.7$.

Both approaches give near the same value for the equivalent gains of the relay and suboptimal controllers. The table reported in the next figure 11 compares the expected values of x_{10} (by DF and LPRS methods) with the values observed in the computer simulations. The difference between the theoretical results and the simulations is due to the relatively large disturbance, which shifts the operating point on the bias function off zero to the point where the slope of the bias function is smaller.

	Relay control	*Suboptimal Control*
X_{10DF}	0.010	0.0045
X_{10LPRS}	0.011	0.0045
X_{10SIM}	0.011	0.0075

Fig. 11. Analysis of average values propagation in the system (53)-(54) with relay and suboptimal control.

Figure 12 makes a different investigation comparing the steady state evolution of x_1 for three different values of the anticipation coefficient β. It shows that by selecting larger and larger values of β it can be achieved a remarkable improvement of performance in terms of higher disturbance suppression due to the increase of the equivalent gain.

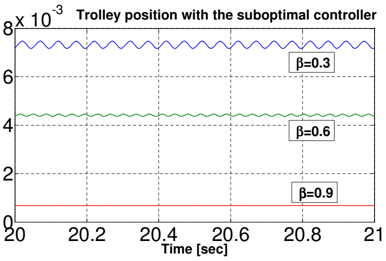

Fig. 12. Trolley position with different values of β

ACKNOWLEDGEMENTS

This work was supported in part by Mexican CONACyT (Consejo Nacional de Ciencia y Tecnologia), grants no. 43807-Y no. J110.418/2006, and Programa de Apoyo a Proyectos de Investigacion e Innovacion Tecnolgica (PAPIIT) UNAM, grant no. 107006-2.

REFERENCES

D.P. Atherton. *Nonlinear Control Engineering - Describing Function Analysis and Design.* Van Nostrand Company Limited, Workingham, Berks, UK, 1975.

G. Bartolini, A. Ferrara, A. Levant, and E. Usai. On Second Order Sliding Mode Controllers. In K.D. Young and U. Ozguner, editors, *Variable Structure Systems, Sliding Mode and Nonlinear Control*, Lecture Notes in Control and Information Sciences, volume 247, pages 329–350. Springer-Verlag, Berlin, 1999.

G. Bartolini, A. Pisano, E. Punta and E. Usai. A survey of applications of second order sliding mode control to mechanical systems. *Int. J. of Control*, 76(9/10): 875–892, 2003.

I. Boiko. Oscillations and transfer properties of relay servo systems The locus of a perturbed relay system approach. *Automatica*, 41(4): 677–683, 2005.

I. Boiko and L. Fridman. Analysis of Chattering in Continuous Sliding-Mode Controllers. *IEEE Transaction on Automatic Control*, 50(9): 1442–1446, 2005.

I. Boiko, L. Fridman, R. Iriarte, A. Pisano and E. Usai. Parameter tuning of second-order sliding mode controllers for linear plants with dynamic actuators. *IEEE Transaction on Automatic Control*, 42: 833–839, 2006.

I. Boiko, L. Fridman, A. Pisano and E. Usai. Analysis of chattering in systems with second order sliding modes. *IEEE Transaction on Automatic Control*, 52: 2085–2102, 2007.

S.V. Emelyanov, S.K. Korovin, and A. Levant. Higher order sliding modes in control systems. *Differential equations*, 29(11): 1627–1647, 1993.

A. Gelb, W.E. VAnder Velde. *Multiple-input describing functions and nonlinear systems design.* Mc-Graw Hill, New York, 1968.

J. T. Hawkins. Automatic regulators for heating apparatus. *Trans. Amer. Soc. Mech. Eng.*, 9: 432, 1887.

A. Levant. Sliding Order and Sliding Accuracy in Sliding Mode Control. *Int. J. of Control*, 58(6): 1247–1263, 1993.

A. Levant. Chattering analysis. *Proc. of the 2007 European Control Conference - ECC '07*, 2007.

Y. B. Shtessel and L. Young-Ju. New approach to chattering analysis in systems with sliding modes. *Proc. of the 1996 IEEE Conference on Decision and Control CDC '96*, 4: 4014-4019, 1996.

Y. B. Shtessel, I. A. Shkolnikov, M.D.J. Brown. An asymptotic second-order smooth sliding mode control. *Asian J. of Control*, 5(4): 498–504, 2003.

Y.Z. Tsypkin. *Relay Control Systems.* Cambridge, UK, 1984.

.